



# Non-hydrothermal synthesis and structure determination of two new $\beta$ -octamolybdate (VI) stabilized with dialkylammonium counterions

Bougar Sarr, Cheikh A.K. Diop, Frederic Melin, Mamadou Sidibe, Petra Hellwig, Francois Michaud, Francis Maury, François Senocq, Abdou Mbaye,  
Yoann Rousselin

## ► To cite this version:

Bougar Sarr, Cheikh A.K. Diop, Frederic Melin, Mamadou Sidibe, Petra Hellwig, et al.. Non-hydrothermal synthesis and structure determination of two new  $\beta$ -octamolybdate (VI) stabilized with dialkylammonium counterions. Journal of Molecular Structure, 2018, 1170, pp.44-50. 10.1016/j.molstruc.2018.05.055 . hal-01829951

HAL Id: hal-01829951

<https://hal.science/hal-01829951>

Submitted on 4 Jul 2018

**HAL** is a multi-disciplinary open access archive for the deposit and dissemination of scientific research documents, whether they are published or not. The documents may come from teaching and research institutions in France or abroad, or from public or private research centers.

L'archive ouverte pluridisciplinaire **HAL**, est destinée au dépôt et à la diffusion de documents scientifiques de niveau recherche, publiés ou non, émanant des établissements d'enseignement et de recherche français ou étrangers, des laboratoires publics ou privés.



## Open Archive TOULOUSE Archive Ouverte (OATAO)

OATAO is an open access repository that collects the work of Toulouse researchers and makes it freely available over the web where possible.

This is an author-deposited version published in : <http://oatao.univ-toulouse.fr/>  
Eprints ID : 20251

**To link to this article :** DOI: 10.1016/j.molstruc.2018.05.055  
URL : <http://doi.org/10.1016/j.molstruc.2018.05.055>

**To cite this version :** Sarr, Bougar and Diop, Cheikh A.K. and Melin, Frederic and Sidibe, Mamadou and Hellwig, Petra and Michaud, Francois and Maury, Francis and Senocq, François and Mbaye, Abdou and Roussel, Yoann *Non-hydrothermal synthesis and structure determination of two new  $\beta$ -octamolybdate (VI) stabilized with dialkylammonium counterions.* (2018) Journal of Molecular Structure, 1170. 44-50. ISSN 0022-2860

Any correspondence concerning this service should be sent to the repository administrator: [staff-oatao@listes-diff.inp-toulouse.fr](mailto:staff-oatao@listes-diff.inp-toulouse.fr)

# Non-hydrothermal synthesis and structure determination of two new $\beta$ -octamolybdate (VI) stabilized with dialkylammonium counterions

Bougar Sarr <sup>a,\*</sup>, Cheikh A.K. Diop <sup>a</sup>, Frederic Melin <sup>b,\*\*</sup>, Mamadou Sidibe <sup>a</sup>, Petra Hellwig <sup>b</sup>, Francois Michaud <sup>c</sup>, Francis Maury <sup>d</sup>, Francois Senocq <sup>d</sup>, Abdou Mbaye <sup>e</sup>, Yoann Roussel <sup>f</sup>

<sup>a</sup> Laboratoire de Chimie Minérale et Analytique (LA.CHI.MIA), Département de Chimie, Faculté des Sciences et Techniques, Université Cheikh Anta Diop, Dakar, Senegal

<sup>b</sup> Chimie de la Matière Complex UMR 7140, Laboratoire de Bioélectrochimie et Spectroscopie, CNRS-Université de Strasbourg, 1 rue Blaise Pascal, 67070, Strasbourg, France

<sup>c</sup> Service commun d'analyse par diffraction des rayons X, Université de Bretagne occidentale, 6, avenue Victor Le Gorgeu, CS 93837, 29238, Brest Cedex 3, France

<sup>d</sup> CIRIMAT, Université de Toulouse, CNRS/INPT/UPS, 4 allée E. Monso, BP 44362, 31030, Toulouse Cedex 4, France

<sup>e</sup> Laboratoire Chimie et Physique des Matériaux (LCPM) de l'Université Assane Seck de Ziguinchor (UASZ), BP: 523, Ziguinchor, Senegal

<sup>f</sup> ICMUB-UMR 6302, 9, avenue Alain Savary, 21000, Dijon, France

## A B S T R A C T

Two new organic–inorganic materials based on Mo–POM, namely  $(^1\text{Pr}_2\text{NH}_2)_2 \cdot ((\text{CH}_3)_2\text{NH}_2)_2 \cdot [\text{Mo}_8\text{O}_{26}]$  (**1**) and  $(\text{Pr}_2\text{NH}_2)_4 \cdot [\text{Mo}_8\text{O}_{26}]$  (**2**), have been synthesized by a non-hydrothermal method at room temperature and characterized by single crystal X-ray diffraction, thermal gravimetric analysis (TGA) and vibrational spectroscopy. The compound (**1**) is a  $\beta$ -[ $\text{Mo}_8\text{O}_{26}$ ]<sup>4-</sup> anion which crystallizes as a mixed salt of both dimethylammonium  $[(\text{CH}_3)_2\text{NH}_2]^+$  and diisopropylammonium  $[^1\text{Pr}_2\text{NH}_2]^+$ . The interaction between anions and cations leads to an inorganic–organic band structure. Similarly, in compound (**2**), the interconnection of  $\beta$ -[ $\text{Mo}_8\text{O}_{26}$ ]<sup>4-</sup> anions with dipropylammonium  $[\text{Pr}_2\text{NH}_2]^+$  cations gives an inorganic–organic band structure. In both compounds, the cations interact with two different sites of the cluster: a fundamental site formed by four highly nucleophilic terminal oxo ligands, and a second site which is composed of  $\text{O}_t$ ,  $\mu_2\text{-O}$  and/or  $\mu_3\text{-O}$  oxygen groups. A remarkable difference between the two compounds is that in compound (**2**) interactions between the bands involve only Van der Waals forces, whereas in compound (**1**) the bands interact also through hydrogen bonds.

**Keywords:**  
 $\beta$ -octamolybdate stabilization  
Hydrogen bonds  
Bifurcated hydrogen bonds  
Crystal structure

## 1. Introduction

Polyoxometalates (POMs) have attracted great attention in recent years due to their tremendous structural variety and special properties [1–3], which enable extensive applications in catalysis, medicine, electronics, electrochemistry, ... [4–6]. POMs decorated with transition metal organic complexes have become a new class of organic–inorganic hybrid materials [7,8]. Polyoxometalates, as one kind of significant metal oxide clusters, have been employed as inorganic building blocks for the construction of supramolecular arrays with various organic compounds [9,10]. The formation mechanism of these compounds, however, is still unknown in the

majority of cases. In the literature POMs are most often synthesized under hydrothermal conditions [11–16], from elementary blocks  $[\text{MO}_x]^{n-}$  ( $\text{M} = \text{Mo, V, W, Ta, Nb}$ ), but the method is limited by serendipity [17,18]. Additionally, in some cases the high temperature required will not retain the structural functionalities of the organic compounds and may be a major drawback during the synthesis.

Octamolybdates (Mo8) are a subclass of the POM family that have been extensively studied due to their diverse structures and interesting properties. To date, nine isomeric forms of octamolybdates have been prepared, namely the  $\alpha$ ,  $\beta$ ,  $\gamma$ ,  $\delta$ ,  $\epsilon$ ,  $\zeta$ ,  $\xi$ ,  $\eta$  and  $\theta$  isomers [19–21]. These isomers are differentiated by the number of tetrahedral ( $\text{MoO}_4$ ), bipyramidal ( $\text{MoO}_5$ ) or octahedral ( $\text{MoO}_6$ ) units contained in their structures. On the basis of density functional theory calculations, the  $\alpha$ - and  $\delta$ -isomers have been predicted to be the most stable and the  $\beta$ -isomer the least stable [22]. A balance

\* Corresponding author.

\*\* Corresponding author.

E-mail addresses: bouks89@gmail.com (B. Sarr), fmelin@unistra.fr (F. Melin).

between unfavorable steric interactions and favorable atomic interactions can account for the relative isomer stabilities. Steric interactions are important in the  $\beta$ -isomer, due to its more compact structure. This isomer can, however, be stabilized by interaction with organic cations. It was suggested that the  $\beta$ -isomer is preferentially formed in the presence of small cations, such as diethylammonium or trimethylsulfonium [23], or in the presence of larger cations having a small electrophilic group which can occupy the sites formed by the two groups of four highly nucleophilic terminal oxo ligands of the cluster [24].

However, we have been able to isolate two new inorganic-organic hybrid compounds, all containing the  $\beta$ -octamolybdate anion with larger secondary ammonium cations. These two compounds, namely  $(^i\text{Pr}_2\text{NH}_2)_2 \cdot ((\text{CH}_3)_2\text{NH}_2)_2 \cdot [\text{Mo}_8\text{O}_{26}]$  and  $(\text{Pr}_2\text{NH}_2)_4 \cdot [\text{Mo}_8\text{O}_{26}]$ , have been synthesized at room-temperature. They provide a more complete picture of the stabilization of  $\beta$ - $[\text{Mo}_8\text{O}_{26}]^{4-}$  through anion-cation interactions.

## 2. Experimental section

### 2.1. Materials

Molybdenum trioxide (85%), ammonium heptamolybdate tetrahydrate, malonic acid (100%), succinic acid (98%), dipropylamine (99%) and diisopropylamine (99%) were purchased from Sigma-Aldrich and used without further purification. Methanol, *N*, *N*-dimethylformamide (DMF) and distilled water were used as solvent.

### 2.2. Synthesis

$(^i\text{Pr}_2\text{NH}_2)_2 \cdot ((\text{CH}_3)_2\text{NH}_2)_2 \cdot [\text{Mo}_8\text{O}_{26}]$  (1): This compound was obtained from a two-step process. First, molybdenum trioxide (3.2 g, 22.2 mmol), malonic acid (2.5 g, 22.2 mmol) and diisopropylamine (8 g, 88.9 mmol) in a ratio of 1:1:4 were dissolved in water. The solution ( $\text{pH} = 4.2$ ) was then stirred for one hour and evaporated in the oven at  $60^\circ\text{C}$  to yield a whitish precipitate. In a second step, recrystallization of this whitish precipitate in DMF leads after 3-weeks slow evaporation at room temperature to pretty white crystals suitable for XRD (24.3% yield).

$(\text{Pr}_2\text{NH}_2)_4 \cdot [\text{Mo}_8\text{O}_{26}]$  (2): similarly to (1) this compound was also obtained from a two-step process. First, ammonium heptamolybdate tetrahydrate (0.78 g, 0.63 mmol), succinic acid (0.15 g, 1.27 mmol) and dipropylamine (0.26 g, 2.54 mmol) in a ratio of 1/2:1:2 were dissolved in water. The solution ( $\text{pH} = 4.5$ ) was then stirred for one hour and evaporated in the oven at  $60^\circ\text{C}$  to yield a greenish precipitate. In a second step, recrystallization of this greenish precipitate in methanol leads after 5-days slow evaporation at room temperature to pretty greenish crystals suitable for XRD (27.2% yield).

### 2.3. Structure determination

Suitable crystals for compounds  $(^i\text{Pr}_2\text{NH}_2)_2 \cdot ((\text{CH}_3)_2\text{NH}_2)_2 \cdot [\text{Mo}_8\text{O}_{26}]$  (1) and  $(\text{Pr}_2\text{NH}_2)_4 \cdot [\text{Mo}_8\text{O}_{26}]$  (2) were measured on a Rigaku Oxford Diffraction SuperNova diffractometer at 293 K at the  $\text{MoK}\alpha$  radiation ( $\lambda = 0.71073 \text{ \AA}$ ). Data collection reduction and multiscan ABSPACK correction were performed with CrysAlisPro (Rigaku Oxford Diffraction). The structure was solved by Patterson method using ShelXT-2015 and refined with SHELXL-2015 [25,26]. Crystallographic Information files were compiled with Olex2.12 [27]. Crystallographic data are summarized in Table 1.

### 2.4. Spectroscopic measurements

The IR spectra were recorded with a Vertex 70 spectrometer from Bruker equipped with a Harrick diamond ATR cell, a globar source and a KBr beamsplitter. 256 scans with  $4 \text{ cm}^{-1}$  resolution were averaged. The final spectra were corrected from the contributions of  $\text{H}_2\text{O}$  and  $\text{CO}_2$  gases.

The Raman spectra was obtained with an Invia Raman Microscope from Renishaw operating at  $\lambda = 514 \text{ nm}$ . Five spectra obtained with 10s irradiation time and 25 mW laser power were averaged.

### 2.5. TGA measurements

Thermogravimetric analysis (TGA) measurement was carried out with a Setaram Sensys Evo under Ar mass flow rate of 20 sccm, from room temperature to  $1000^\circ\text{C}$  with a heating rate of  $10^\circ\text{C} \cdot \text{min}^{-1}$ . These conditions allow to study only the thermal stability under inert gas and not the degradation by reaction at high temperature in an oxidizing medium (in air for example), which would be more complex. The test portion of each product was between 14 and 24 mg. The return to ambient temperature ( $25^\circ\text{C}$ ) from the  $1000^\circ\text{C}$  at the end of the analysis was made with a negative temperature ramp of  $-33^\circ\text{C} \cdot \text{min}^{-1}$ .

## 3. Results and discussion

### 3.1. Discussion of synthesis

The compounds (1) and (2) were prepared by a gentle route from the  $\text{MoO}_3$  and  $(\text{NH}_4)_6\text{Mo}_7\text{O}_{24} \cdot 4\text{H}_2\text{O}$  precursors, respectively. Suspending  $\text{MoO}_3$  in water immediately causes the formation of molybdic acid ( $\text{H}_2\text{MoO}_4$ ). The formation of the compound (1) is based on a self-assembly reaction via acid-base polycondensation processes. In addition, since dimethylamine was not listed in the reagent list, the presence of the dimethylammonium cation in the compound could be surprising. Indeed, the dimethylammonium present in the compound comes from transformation of DMF to dimethylamine with release of formic acid. And as soon as the dimethylamine is formed in the medium it protonates to lead to dimethylammonium. The formation of the compound (2) involves the conversion of a  $[\text{Mo}_7\text{O}_{24}]^{6-}$  anion into a  $\beta$ - $[\text{Mo}_8\text{O}_{26}]^{4-}$  one according to the reported acid-base equilibrium [28]. Malonic acid (compound 1) and succinic acid (compound 2) were used to work in an acidic reaction medium, since the polyoxometalates are usually obtained by acidifying the medium ( $\text{pH} < 7$ ). If the medium is not acidified, mononuclear compounds are usually obtained ( $[\text{MoO}_4]^{2-}$ ).

### 3.2. Structure description and discussion

In both compounds, the cluster consists of eight distorted  $\text{MoO}_6$  octahedra sharing corners and edges forming thus a  $\beta$ - $[\text{Mo}_8\text{O}_{26}]^{4-}$  anion (Fig. 1). The complete octamolybdate anion is generated by a crystallographic inversion centre. The  $[\text{Mo}_8\text{O}_{26}]^{4-}$  anion of compound (1) crystallizes as a mixed salt of dimethylammonium  $[(\text{CH}_3)_2\text{NH}_2]^+$  and diisopropylammonium  $[^i\text{Pr}_2\text{NH}_2]^+$  in a triclinic system of P-1 space group. Its asymmetric unit consists of one half  $\beta$ - $[\text{Mo}_8\text{O}_{26}]^{4-}$  cluster anion, one  $[(\text{CH}_3)_2\text{NH}_2]^+$  and one  $[^i\text{Pr}_2\text{NH}_2]^+$  cations. Compound (2) also crystallizes in the triclinic space group P-1, and its asymmetric unit consists of one half  $\beta$ - $[\text{Mo}_8\text{O}_{26}]^{4-}$  cluster anion and two  $[\text{Pr}_2\text{NH}_2]^+$  cations. In  $[\text{Mo}_8\text{O}_{26}]^{4-}$  clusters we usually distinguish four different types of oxygen atoms: the  $\text{O}_{\text{t}}$  (terminal oxygen atoms), the  $\mu 2-\text{O}$  (oxygens bridging two molybdenum atoms), the  $\mu 3-\text{O}$  (oxygens bridging three molybdenum

**Table 1**  
Crystallographic data of compounds 1 and 2.

Compound	(1)	(2)
Formula weight (g.mol <sup>-1</sup> )	1480.10	1592.30
Crystal system	Triclinic	Triclinic
Space group	P-1	P-1
a (Å)	8.3232 (4)	10.5178 (4)
b(Å)	10.6040 (5)	10.7854 (6)
c(Å)	11.9289 (6)	11.9783 (7)
$\alpha(^{\circ})$	102.837 (2)	78.312 (5)
$\beta(^{\circ})$	97.027 (2)	84.537 (4)
$\gamma(^{\circ})$	105.085 (2)	65.019 (5)
V (Å <sup>3</sup> )	972.83 (8)	1206.07 (12)
Z	1	2
Temperature (K)	100	293
$\mu(\text{mm}^{-1})$	2.58	2.09
Crystal size (mm <sup>3</sup> )	0.30 × 0.20 × 0.14	0.14 × 0.14 × 0.08
R1 [ $I = 2\sigma(I)$ ]	0.029	0.042
wR2 [ $I = 2\sigma(I)$ ]	0.069	0.100
Radiation	Mo K $\alpha$ radiation ( $\lambda = 0.71073 \text{ \AA}$ )	Mo K $\alpha$ radiation ( $\lambda = 0.71073 \text{ \AA}$ )
2 $\theta$ range for data collection (°)	3.3 to 27.5	3.7 to 26.9
hkl range	$-10 \leq h \leq 10; -13 \leq k \leq 13; -15 \leq l \leq 15$	$-13 \leq h \leq 13; -14 \leq k \leq 14; -15 \leq l \leq 15$
Reflections collected	25776	71641
Independent reflections	4472 [ $R_{\text{int}} = 0.021$ ]	5492 [ $R_{\text{int}} = 0.085$ ]
Goodness-of-fit on $F^2$	1.34	1.05
Largest diff. peak and hole (e Å <sup>-3</sup> )	0.69/-1.04	0.88; -0.69

atoms) and the  $\mu_5\text{-O}$  (oxygens bridging five molybdenum atoms) (Fig. 1 and Table 2). The variation of Mo–O bond lengths in the  $[\text{Mo}_8\text{O}_{26}]^{4-}$  polyanion is a function of the type of oxygen atom brought into play. In compound (1), these Mo–O bond lengths vary between 1.691 (3)-1.719 (3) Å for the  $\text{Ot}$ , 1.764 (3)-2.278 (3) Å for the  $\mu_2\text{-O}$ , 1.952 (3)-2.330 (3) Å for the  $\mu_3\text{-O}$  and 2.146 (3)-2.435 (3) Å for the  $\mu_5\text{-O}$ . In compound (2), these Mo–O bond lengths vary

between 1.689 (4)-1.709 (4) Å for the  $\text{Ot}$ , 1.749 (3)-2.290 (3) Å for the  $\mu_2\text{-O}$ , 1.946 (3)-2.351 (3) Å for the  $\mu_3\text{-O}$  and 2.142 (3)-2.460 (3) Å for the  $\mu_5\text{-O}$ . Overall, the Mo–O lengths and O–Mo–O angles found here are consistent with  $\beta\text{-}[\text{Mo}_8\text{O}_{26}]^{4-}$  anions previously reported [24,29–32] and show that the  $\text{MoO}_6$  octahedra are deformed.

The involvement of terminal oxides in hydrogen bonding is likely to result in lengthening of the Mo–O bonds. We note, however, that the Mo–Ot still exhibit the shortest lengths. In addition, for both compounds (1) and (2) the Mo–O bonds are generally longer in the case of  $\mu_3\text{-O}$  [ $\mu_3\text{-O-Mo}$  (max) = 2.323 (3) Å for (1) and 2.350 (3) Å for (2)], but even longer in the case of  $\mu_5\text{-O}$  [ $\mu_5\text{-O-Mo}$  (max) = 2.435 (3) Å for (1) and 2.460 (3) Å for (2)]. This was also reported in the literature for similar compounds but was not yet interpreted [33,34]. We suggest here that some variations in the Mo–O bond lengths in the  $\beta\text{-}[\text{Mo}_8\text{O}_{26}]^{4-}$  cluster can be explained at least partially by the fact that the junction of two  $\text{MoO}_6$  octahedra by edge sharing brings the two positive ( $\text{Mo}^{\text{VI}+}$ ) ions closer, which enhances their mutual repulsive interaction (Coulomb interaction). This favors a stretching of the equatorial Mo–O bond lengths involved. For compound (1), this is the case for the octahedrons of adjacent metal centers such as ( $\text{Mo}_2$ ,  $\text{Mo}_4$ ) where  $[\text{Mo}_4\text{-O}_3\text{i}(\mu_2)] = 2.278$  (3) Å,  $\text{Mo}_2\text{-O}_1\text{i}(\mu_5) = (\mu_5)\text{O}_1\text{i}\text{-Mo}_2\text{i} = 2.363$  (3) Å,  $\text{Mo}_4\text{-O}_1\text{i}(\mu_5) = 2.435$  (3) Å, ( $\text{Mo}_2$ ,  $\text{Mo}_2$ ) where  $[\text{Mo}_2\text{-O}_1\text{i}(\mu_5) = (\mu_5)\text{O}_1\text{i}\text{-Mo}_2\text{i} = 2.363$  (3) Å], ( $\text{Mo}_1$ ,  $\text{Mo}_3$ ) where  $[\text{Mo}_3\text{-O}_4(\mu_3) = 2.001$  (2) Å,  $\text{Mo}_3\text{-O}_2\text{i}(\mu_3) = 2.323$  (3) Å,  $\text{Mo}_1\text{-O}_4\text{i}(\mu_3) = 2.330$  (3) Å], ...

In spite of the steric hindrance of secondary ammonium groups, two of them remain in interaction with the two groups of highly nucleophilic  $\text{Ot}$  ( $\text{O}_9$ ,  $\text{O}_{10}$ ,  $\text{O}_{11}$ ,  $\text{O}_{12}$ ) of the cluster (Figs. 1 and 2). This site of interaction has been suggested previously to be fundamental for the stabilization of the  $\beta$ -isomer [24,35]. In addition, we observe that secondary ammonium groups are also able to interact with different sites of the cluster, which involve  $\text{Ot}$ , and  $\mu_2\text{-O}$  in compound (1) and  $\text{Ot}$ ,  $\mu_2\text{-O}$  and  $\mu_3\text{-O}$  oxygen groups in compound (2) (Fig. 3). Between these two different sites of interaction, it is very difficult to specify the preferred one favoring the formation of the  $\beta$ -isomer.

In our compounds we have more cations in the second type of site (6 in compound (1) and 4 in compound (2) (Fig. 3)) than in the

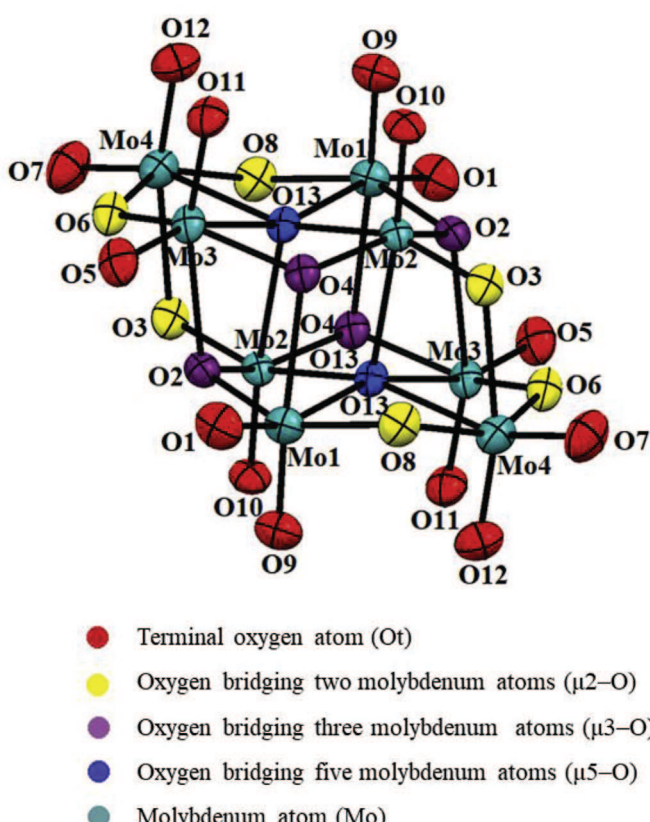


Fig. 1. Cluster representation  $\beta\text{-}[\text{Mo}_8\text{O}_{26}]^{4-}$ .

**Table 2**  
 $\beta$ -octamolybdate oxygens involved in hydrogen bonds.

Types of oxygen atoms	Number of oxygen atoms involved in Hydrogen bonds (1)	Number of oxygen atoms involved in Hydrogen bonds (2)
Ot (14 in number)	8 (O1, O7, O11, O12)	8 (O5, O9, O11, O12)
$\mu$ 2–O (6 in number)	2 (O3)	2 (O6)
$\mu$ 3–O (4 in number)	0	2 (O2)
$\mu$ 5–O (2 in number)	0	0

fundamental site. We thus observe here that all types of oxygen except  $\mu$ 5–O are able to interact with a cation to stabilize the  $\beta$ -isomer (Table 2). Due to the trapping of the  $\mu$ 5–O atoms at the heart of the cluster and due to the number of links they already have, it is very unlikely for them to interact with a cation.

We add that in both compounds, for each  $[\text{Mo}_8\text{O}_{26}]^{4-}$  anion, cations occupy crystallographic sites so as to perform centrosymmetric cation-anion-cation interactions (Figs. 2 and 3). Moreover, it is these centrosymmetric interactions that allow most of compounds with  $\beta$ -octamolybdate anion to crystallize with a P-1 space-group. Indeed, lesser centrosymmetric interactions could lead to anion distortion, or even a break of M–O bonds. This leads to a lowering of symmetry and gives other isomers (for example change from an Oh to a TD or from an Oh to a BPT).

In compound (1), each  $\beta$ -octamolybdate anion connects to two neighbors via two diisopropylammonium cations (Fig. 4a). These interactions involve two “parallel” hydrogen bonds N1–H1A···O1 (2.919 (4) Å) and N1–H1A···O7 (2.942 (4) Å), all involving Ot. This leads to an infinite band. In addition, through the other cation, dimethylammonium, these infinite bands interact through bifurcated hydrogen bonds N2–H2E···(O11, O12) (3.099 (5) Å, 3.015 (5) Å) on one side and simple hydrogen bonds N2–H2D···O3 (3.211 (5) Å) on the other side leading to an infinite layer structure. Similarly for compound (2), the anions are bridged by two propylammonium ions via simple N1–H1B···O5 (2.886 (6) Å) and bifurcated

N1–H1A···(O2, O6) (3.281 Å, 3.031 Å) hydrogen bonds, which leads to an infinite band (Fig. 4a). The two remaining cations interact laterally with the polyanion via simple N2–H2C···O11 (2.953 (7) Å) and bifurcated N2–H2C···(O9, O12) (2.988 (6) Å, 2.988 Å) hydrogen bonds, which leaves no available hydrogen for further interaction. The 2D structure of both compounds thus consists of infinite bands where anions and cations alternate. The bands of the compound (2) interact with each other only via Van der waals interaction (Fig. 4b), whereas hydrogen bonds are also involved in the interaction between the bands in compound (1) (Fig. 4a).

### 3.3. Thermal analyses

The thermal stability of compounds 1 and 2 was determined by TGA. In Fig. 5a is shown the diagram of compound (1). Between 0° and 1000 °C the curve indicates a total mass loss of the order of 80% in several stages, reflecting a complex mechanism of degradation of the compound. At the end of the TGA analysis a black solid residue was observed in the crucible. It could be a mixture of  $\text{MoO}_2$  as the main phase since it is the most stable phase of the Mo–O system with a melting point higher than 2100 °C [36] and other byproducts as secondary phases including Mo, Magnéli phases (mixed-valence oxides) or molybdenum carbide. TGA analysis confirms that the compound is anhydrous since up to 250 °C there was no loss of mass that could be assimilated to departure of water molecules. A first rapid mass loss of about 20% corresponding to the departure of the four cations, i.e. 2  $[\text{iPr}_2\text{NH}_2]^+$  and 2  $[(\text{CH}_3)_2\text{NH}_2]^+$  (20.1% calculated) is observed in the 250–370 °C range. A more detailed analysis indicates that this first mass loss of about 20% is done in two steps: (i) about 15% from 250 to 300 °C then 5% from 300 to 370 °C. This could correspond to the departure of the two  $[\text{iPr}_2\text{NH}_2]^+$  (13.8% calculated) first then the two  $[(\text{CH}_3)_2\text{NH}_2]^+$  (6.2% calculated). This result would reveal a higher thermal stability of the dimethylammonium salt compare to the

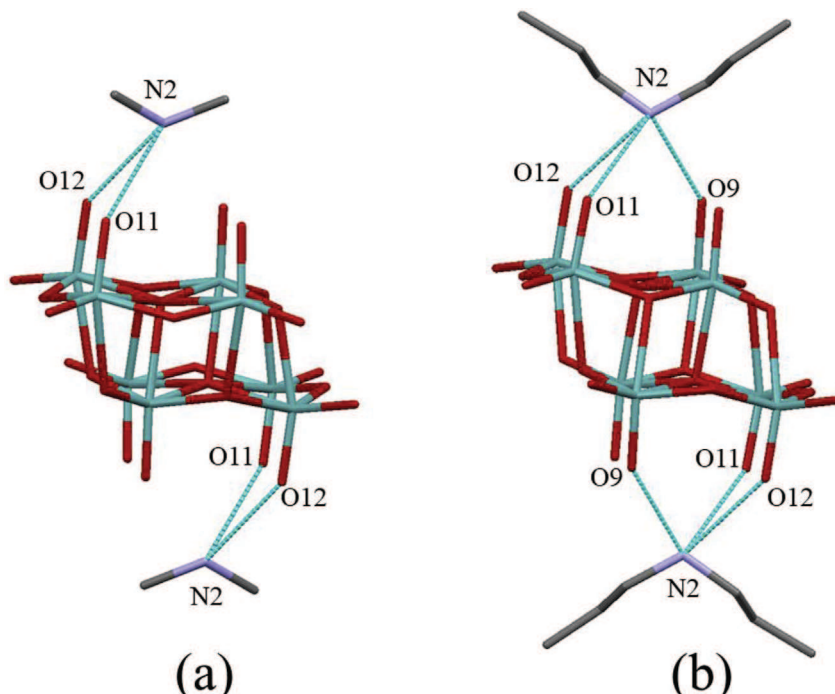


**Fig. 2.** View of the interactions between  $\beta$ -[ $\text{Mo}_8\text{O}_{26}]^{4-}$  anion and the cations located in the fundamental site (highly nucleophilic) [24]: (a) compound (1) and (b) compound (2). Hydrogen atoms are omitted for clarity.

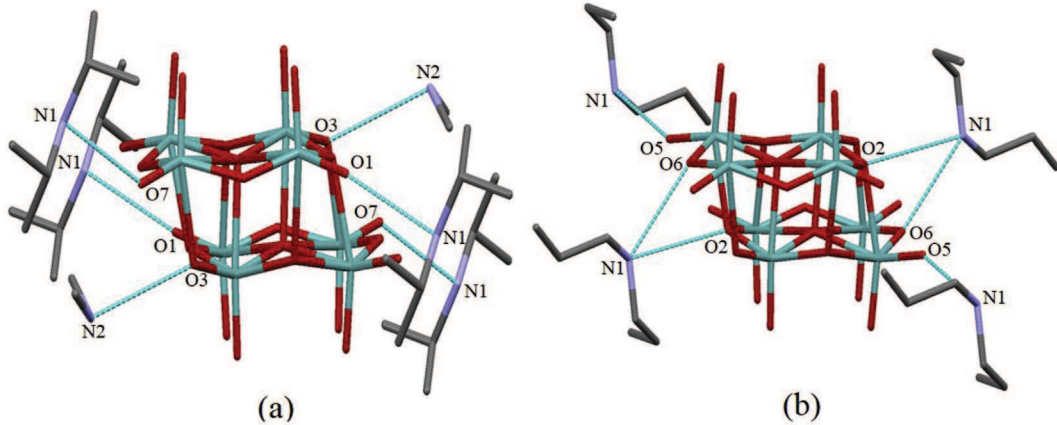


**Fig. 3.** View of the interactions between  $\beta$ -[Mo<sub>8</sub>O<sub>26</sub>]<sup>4-</sup> anion and the cations located outside the fundamental site: a) compound (1) and b) compound (2). Hydrogen atoms are omitted for clarity.

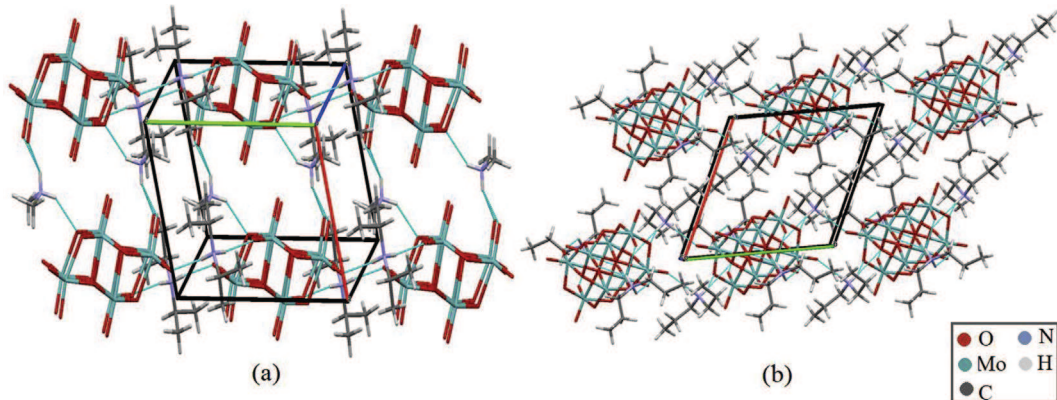


**Fig. 4.** Supramolecular assembly of cations and anions in the layers of compound 1 (a) and compound (2) (b).

diisopropylammonium one in this compound family. Once released the organic part of the compound (1), the rest of the curve corresponds to the decomposition of the inorganic  $\beta$ -octamolybdate anion.

Thus, a second rather slow mass loss of about 7% occurs in the 370–620 °C range corresponding to a first degradation of the polyanion with departure of either one MoO<sub>3</sub> entity (9.7% calculated) or three O<sub>2</sub> molecules (6.5% calculated). The first hypothesis for this step, *i.e.* vaporization of MoO<sub>3</sub>, is supported by the high vapor pressure of MoO<sub>3</sub> that is higher than 10<sup>-2</sup> Torr at 620 °C [37]. At this stage, such a decomposition pathway of  $\beta$ -[Mo<sub>8</sub>O<sub>26</sub>]<sup>4-</sup> should leave metastable mixed-valence oxides as Mo<sub>4</sub>O<sub>11</sub> that have been reported stable until 607 °C [37], which is in good agreement with the limit of 620 °C where a further step occur. However this is perhaps not the most likely way because when pure MoO<sub>3</sub> is sublimated it vaporizes in the form of a trimer (MoO<sub>3</sub>)<sub>3</sub> and if it was also the case from  $\beta$ -[Mo<sub>8</sub>O<sub>26</sub>]<sup>4-</sup> then the experimental mass loss would not correspond. A second hypothesis for this step would be the release of O<sub>2</sub> molecules, which should leave solid oxides again as Mo<sub>4</sub>O<sub>11</sub> and also Mo<sub>8</sub>O<sub>23</sub> that is stable up to 775 °C [36]. A third loss of mass of about 20% between 620 and 820 °C can be attributed to the release of two MoO<sub>3</sub> molecules (19.5% calculated). The melting point of MoO<sub>3</sub> being at 800 °C [36] the mass loss is relatively fast in this temperature range. In this third step, MoO<sub>3</sub> may originate from the disproportionation (i) of Mo<sub>4</sub>O<sub>11</sub>, which forms above 607 °C MoO<sub>3</sub> gas and Mo<sub>2</sub>O<sub>5</sub> solid [37], and (ii) of Mo<sub>8</sub>O<sub>23</sub> that produces above 775 °C MoO<sub>3</sub> gas and Mo<sub>4</sub>O<sub>11</sub> which in turn will form MoO<sub>2</sub>

[36].

The complete degradation of the polyanion occurs in the last step above 820 °C by releasing oxygen and MoO<sub>3</sub> molecules and leaving a solid residue probably constituted of MoO<sub>2</sub> that are the most refractory materials of this chemical system and traces of other byproducts as Mo which is thermodynamically stable with MoO<sub>2</sub> [36] and possibly molybdenum carbide due to the presence of organic ligands.

The TGA curve of the compound (2) is given in Fig. 5b. There are similarities in the two curves of Fig. 5 but also some differences. The departure of the organic part is clearly visible at low temperature starting from 220 °C to 350 °C with a total mass loss of about 25% (25.6% calculated for 4 [Pr<sub>2</sub>NH<sub>2</sub>]<sup>+</sup>). More precisely two steps occur in this temperature range; from 220 to 275 °C with a mass loss of 12% and the second from 275 to 350 °C with a mass loss of 13%. Each step corresponds to the same mass loss, which means that each corresponds to the departure of two [Pr<sub>2</sub>NH<sub>2</sub>]<sup>+</sup> perhaps by a concerted mechanism. It is remarkable that [Pr<sub>2</sub>NH<sub>2</sub>]<sup>+</sup> cations leave in the same temperature range as the ammonium cations of the compound (1): 220–350 °C and 250–370 °C for compounds (2) and (1) respectively.

Then the decomposition of the inorganic polyanion occurs in two stages. From 350 to about 880 °C a slow process leads to a mass loss of about 12%, which could correspond mainly to the release of one MoO<sub>3</sub> (9.1% calculated). A slight change in slope occurs around 800 °C due to the melting of MoO<sub>3</sub> and thus to a variation in its release rate. Such a decomposition by a release of MoO<sub>3</sub> in this

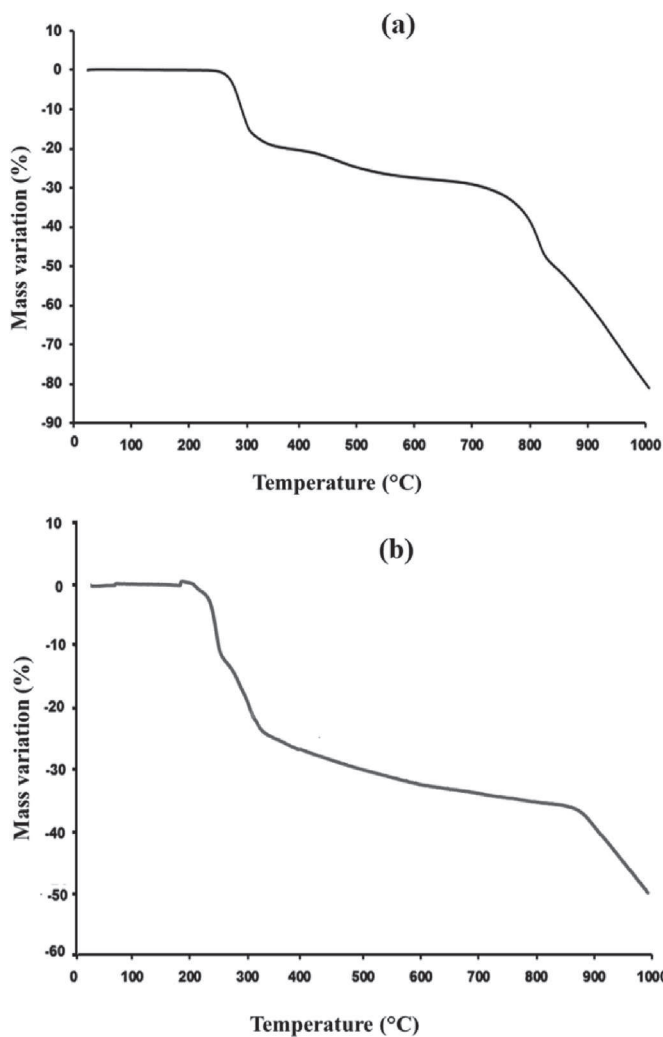


**Fig. 5.** TGA diagrams of compound 1 (a) and compound (2) (b).

temperature range 350–880 °C for compound (2) is likely very similar to that observed in almost the same range 370–820 °C for compound (1), which means it occurs by leaving mixed-valence oxides as  $\text{Mo}_4\text{O}_{11}$  and  $\text{Mo}_8\text{O}_{23}$  which have been reported stable up to 607 °C [37] and 775 °C [36], respectively. Beyond 880 °C for compound (2) and 820 °C for compound (1) a faster and continuous degradation mechanism occurs, which probably leaves essentially  $\text{MoO}_2$  as solid residue at 1000 °C.

Interestingly, a major difference between compound (1) and (2) is found in their behavior at high temperature. The above analysis suggests that up to about 820 °C for compound (1) and 880 °C for compound (2) the decomposition mechanism is very similar, with the departure of ammonium cations first, then the first molecules of  $\text{MoO}_3$  and  $\text{O}_2$  directly from the polyanion with the formation of mixed-valence oxides, which in turn liberate  $\text{MoO}_3$  leaving  $\text{MoO}_2$  which is stable at very high temperature. The fact that the losses of mass both up to this temperature threshold and at the end of the analysis at 1000 °C is 50% and 80% for the compounds (1) and 37% and 50% for the compound (2) indicates a higher thermal stability of the compound (2), which would leave a higher amount of  $\text{MoO}_2$  as solid residue at 1000 °C. Probably this result can be related to the difference of anion-cation interactions on the level of the fundamental sites of stabilization [24]. In the compound (2) the anion-cation interactions involving the fundamental sites (Fig. 2b) being done by simple and bifurcated hydrogen bonds, are much stronger

than in the compound (1) where they are done by only a bifurcated hydrogen bond (Fig. 2a). These strong interactions on the level of fundamental sites (Fig. 2b) tend to increase the symmetry and the stability of the  $\beta$ -octamolybdate in the compound (2) furthering thus its thermal stability. As the polyanion is symmetric with lengths and angles bond well defined, the departure of the cations won't probably modify the architecture and the symmetry of the polyanion owing to the presence of strong Mo–O bonds. Unfortunately, at this stage, the amount of solid residue after TGA of both compounds was too small to be analyzed by XRD and to strongly support this discussion.

### 3.4. IR spectra

The mid infrared spectra (Fig. S1, in Supplementary information) are dominated by the characteristic absorption bands of the  $[\text{Mo}_8\text{O}_{26}]^{4-}$  cluster in the 1000–650  $\text{cm}^{-1}$  range. The high similarity of the two spectra in this range confirms that the two compounds share a common cluster structure. Compound (2) exhibits two very intense bands at 943 and 899  $\text{cm}^{-1}$  which can be attributed to  $\nu_{\text{antisym}}$  ( $\text{Mo}-\text{O}$ ) stretching vibrations and two more bands at 839 and 687  $\text{cm}^{-1}$  where the  $\nu(\text{Mo}-\langle\mu-\text{O}\rangle)$  and  $\nu(\text{Mo}-\text{O}-\text{Mo})$  vibrations are expected to contribute [38,39]. The corresponding bands are observed at 942, 898, 835 and 704  $\text{cm}^{-1}$  for compound (1). The splitting of the bands at 898 and 835  $\text{cm}^{-1}$  suggests that in compound (1) the  $\beta$ - $[\text{Mo}_8\text{O}_{26}]^{4-}$  cluster is less symmetric/or more distorted than in compound (2) which can be due to its interaction with two different cations. This symmetry defect of  $\beta$ - $[\text{Mo}_8\text{O}_{26}]^{4-}$  in the compound (1) causes a diminution of its stability. That was confirmed furthermore by the thermal analysis.

At higher wavenumbers the bending N–H (1400–1100  $\text{cm}^{-1}$  range), the C–H stretching (3000–2700  $\text{cm}^{-1}$  range) and the N–H stretching modes (above 3000  $\text{cm}^{-1}$ ) of the secondary ammonium cations can be observed.

### 3.5. Raman spectra

Raman spectroscopy is an appropriate and highly efficient tool for the identification of POM compounds in particular for the discrimination of the different isomers of octamolybdate anions [40]. Again the 1000–600  $\text{cm}^{-1}$  is the most informative region. The Raman spectrum of compound (1) (Fig. S2, in Supporting information) exhibits bands at 965, 943, 922 and 893  $\text{cm}^{-1}$  which can be attributed to  $\nu(\text{Mo}-\text{O})$  vibrations. In contrast to IR spectroscopy, the most intense band at 965  $\text{cm}^{-1}$  corresponds to a symmetric stretching mode. At lower wavenumbers (835 and 804  $\text{cm}^{-1}$ ) are expected the contributions of the  $\nu(\text{Mo}-\text{O}-\text{Mo})$  modes. The position of these latter bands is consistent with a  $\beta$ -isomer [40]. For compound (2) (Fig. S2, in Supporting information), the corresponding bands are found at 967, 946, 925, 907 and 838  $\text{cm}^{-1}$ .

## 4. Conclusion

Two new octamolybdate-based hybrid compounds have been synthesized by non-hydrothermal conditions at room temperature and structurally characterized. The structures of compounds have been established by single-crystal X-ray diffraction and also characterized by IR spectroscopy, Raman spectroscopy and TG analysis. The  $\beta$ -octamolybdate structure is stabilized by cation-anion interactions involving the  $\text{O}$ ,  $\mu_2-\text{O}$  and/or  $\mu_3-\text{O}$  oxygen atoms of the cluster. The compounds exhibit good thermal stability. However, due to the difference of anion-cation interactions on the level of the fundamental sites of stabilization, the polyanion of compound (2) is appreciably more stable than that of compound (1). Furthermore, we note that the formation of  $\beta$ -octamolybdate is possible with

both small cations and large cations and all types of oxygen can be involved in hydrogen bonds with the cation except  $\mu$ 5-O. This work is important in directing the design and synthesis of POMs based products with desired properties. It could also open up a new synthesis route to conducting functional materials.

## Acknowledgments

The authors thank the Université Cheikh Anta Diop, Dakar, Senegal, the CNRS and Université de Strasbourg, France, the Université de Bretagne Occidentale, Service Commun d'Analyse par Diffraction des Rayons X, France, the Faculté des sciences-Aix Marseille Université, Marseille, France and the ICMUB-UMR 6302, 9, avenue Alain Savary 21000 DIJON, FRANCE for financial support. All measurements except the TGA were performed in the institutes above quoted. The authors acknowledge also Cédric Charvillat for technical assistance in TGA analyses.

## Appendix A. Supplementary data

Supplementary data related to this article can be found at <https://doi.org/10.1016/j.molstruc.2018.05.055>.

## References

- [1] Y.Q. Jiao, M.T. Li, C. Qin, Z.M. Su, CrystEngComm 19 (2017) 1721.
- [2] B.C. Yin, B. Wu, E. Mamontov, LL. Daemen, Y.Q. Cheng, T. Li, S. Seifert, K.L. Hong, P.V. Bonnesen, J.K. Keum, A.J. Ramirez-Cuesta, J. Am. Chem. Soc. 138 (2016) 2638.
- [3] L.P. Ji, J. Du, J.S. Li, L.C. Zhang, X.J. Sang, H. Yang, H.J. Cui, Z.M. Zhu, RSC Adv. 6 (2016) 28956.
- [4] A. Chieregato, J.M. López Nieto, F. Cavani, Coord. Chem. Rev. 301 (2014) 3.
- [5] C.S. Ayingone Mezui, P.D. Oliveira, A.L. Teillout, J. Marrot, P. Berthet, M. Lebrini, I.M. Mbomekallé, Inorg. Chem. 56 (2017) 1999.
- [6] M.F. Zhang, J.C. Hao, A. Neyman, Y.F. Wang, I.A. Weinstock, Inorg. Chem. 56 (2017) 2400.
- [7] A.X. Tian, Y. Tian, Y.L. Ning, X. Hou, H.P. Ni, X.B. Ji, G.C. Liu, J. Ying, Dalton Trans. 45 (2016) 13925.
- [8] A.X. Tian, J. Ying, J. Peng, J.Q. Sha, Z.M. Su, H.J. Pang, P.P. Zhang, Y. Chen, M. Zhu, Y. Shen, Cryst. Growth Des. 10 (2010) 1104.
- [9] Y.Q. Lan, S.L. Li, X.L. Wang, K.Z. Shao, D.Y. Du, H.Y. Zang, Z.M. Su, Inorg. Chem. 47 (2008) 8179.
- [10] Y. Ding, J.X. Meng, W.L. Chen, E.B. Wang, CrystEngComm 13 (2011) 2687.
- [11] S. Li, L. Zhang, H. Ma, H. Pang, J. Chem. Sci. DOI 10.1007/s12039-016-1076-2.
- [12] X.-Y. Wu, W.-B. Yang, W.-M. Wu, J.-Z. Liao, S.-S. Wang, C.-Z. Lu, Inorg. Chem. Commun. 76 (2017) 118.
- [13] Y.-Q. Zhang, C.-C. Wang, T. Zhu, P. Wang, S.-J. Gao, R. Soc. Chem. 5 (2015) 45688.
- [14] X.-D. Du, C.-C. Wang, J. Zhong, J.-G. Liu, Y.-X. Li, P. Wang, J. Environ. Chem. Eng. 5 (2017) 1866.
- [15] X. Wang, S. Zhang, X. Wang, G. Liu, H. Lin, H. Zhang, Dalton Trans. 46 (2017) 16580.
- [16] C. Gong, X. Zeng, C. Zhu, J. Shu, P. Xiao, H. Xu, L. Liu, J. Zhang, Q. Zeng, J. Xie, RSC Adv. 6 (2016), 106248.
- [17] K. Oshihara, Y. Nakamura, M. Sakuma, W. Ueda, Catal. Today 71 (2001) 153.
- [18] A. Dolbecq, F. Secheresse, Adv. Inorg. Chem. 53 (2002) 1.
- [19] X.D. Du, C.H. Li, Z. Zhang, S. Liu, Y. Ma, X.Z. You, CrystEngComm 13 (2011) 2350.
- [20] D.G. Allis, E. Burkholder, J. Zubietta, Polyhedron 23 (2004) 1145.
- [21] D.G. Allis, R.S. Rarig, E. Burkholder, J. Zubietta, J. Mol. Struct. 688 (2004) 11.
- [22] A.J. Bridgeman, J. Phys. Chem. A 106 (2002) 12151. <https://pubs.acs.org/doi/abs/10.1021/jp027037l?journalCode=jpcagh/jp027037IAF1>.
- [23] W. Xin, X.X. Xiang, W. Ying, Z.Y. Li, J. Inorg. Organom. Chem. 11 (1992) 1423.
- [24] A.B. Kama, R. Dessapt, H. Serier-Brault, M. Sidibe, C.A.K. Diop, R. Gautier, J. Mol. Struct. 1141 (2017) 698.
- [25] G.M. Sheldrick, Acta Cryst. A 71 (2015) 3.
- [26] G.M. Sheldrick, Acta Cryst. C 71 (2015) 3.
- [27] O.V. Dolomanov, L.J. Bourhis, R.J. Gildea, J.A.K. Howard, H. Puschmann, J. Appl. Crystallogr. 42 (2009) 339.
- [28] S. Li, L. Zhang, H. Ma, H. Pang, J. Chem. Sci. DOI 10.1007/s12039-016-1076-2.
- [29] M. Hajji, M.F. Zid, A. Driss, Acta Cryst. E 65 (2009) i21.
- [30] R. Ksiksi, M. Graia, A. Driss, J. Soc. Chim. Tunisie 9 (2007) 71.
- [31] S. Ben Hila, M.F. Zid, A. Driss, Acta Cryst. E 65 (2009) i11.
- [32] T.R. Amarante, I.S. Gonçalves, F.A. Almeida Paz, Acta Cryst. E 71 (2015) m244.
- [33] T.R. Amarante, I.S. Gonçalves, F.A. Almeida Paz, Acta Cryst. E 71 (2015) m244.
- [34] I. Zebiri, S. Boufas, S. Mosbah, L. Bencharif, M. Bencharif, J. Chem. Sci. DOI 10.1007/s12039-015-0948-1.
- [35] W. Xin, X.X. Xiang, W. Ying, Z.Y. Li, J. Inorg. Organom. Chem. 11 (1992) 1423.
- [36] L. Brewer, R.H. Lamoreaux, Bull. Alloy Phase Diagrams 1 (1980) 85–89.
- [37] P.E. Blackburmn, M. Hoch, H.L. Johnston, J. Phys. Chem. 62 (1958) 769–773.
- [38] W.G. Klemperer, W. Shum, J. Am. Chem. Soc. 98 (1976) 8291.
- [39] M. Ayed, S. Thabet, A. Haddad, J. Inorg. Organomet. Polym. 24 (2014) 291.
- [40] D. Rémi, D. Kervern, M. Bujoli-Doeuff, P. Deniard, M. Evain, S. Jobic, Inorg. Chem. 49 (2010) 11309.